AJNR

Diffusion Tensor Imaging in Joubert Syndrome

A. Poretti, E. Boltshauser, T. Loenneker, E.M. Valente, F. Brancati, K. Il'Yasov and T.A.G.M. Huisman

AJNR Am J Neuroradiol 2007, 28 (10) 1929-1933
doi: https://doi.org/10.3174/ajnr.A0703
http://www.ajnr.org/content/28/10/1929

ORIGINAL RESEARCH

Diffusion Tensor Imaging in Joubert Syndrome

A. Poretti
E. Boltshauser
T. Loenneker
E.M. Valente
F. Brancati
K. Il'Yasov
T.A.G.M. Huisman

BACKGROUND AND PURPOSE: Neuropathologic findings and preliminary imaging studies demonstrated the absence of pyramidal tract and superior cerebellar peduncular decussation in individual patients with Joubert syndrome (JS). We hypothesized that functional-structural neuroimaging findings do not differ between the genetic forms of JS.

MATERIALS AND METHODS: MR imaging was performed with a 3T MR imaging-unit. Multiplanar T2- and T1-weighted imaging was followed by diffusion tensor imaging (DTI). Isotropic diffusion-weighted images, apparent diffusion coefficient maps, and color-coded fractional anisotropy maps, including tractography, were subsequently calculated.

RESULTS: In all 6 patients studied, DTI showed that the fibers of the superior cerebellar peduncles did not decussate in the mesencephalon and the corticospinal tract failed to cross in the caudal medulla. The patients represented various genetic forms of JS.

CONCLUSION: In JS, the fibers of the pyramidal tract and the superior cerebellar peduncles do not cross, irrespective of the underlying mutation.

Joubert syndrome (JS) is an autosomal-recessive disorder presenting with hypotonia, ataxia, developmental delay, mental retardation, irregular breathing in the neonatal period, and ocular motor apraxia.[1,2] Involvement of the kidneys (nephronophthisis), liver (fibrosis), and eyes (mostly as retinal dystrophy but also as ocular colobomas) are features associated with JS.[3,4] The key neuroradiologic hallmarks of JS include cerebellar vermis hypoplasia in combination with the "molar tooth sign" (MTS), a complex malformation of the midbrain characterized by thickened and elongated superior cerebellar peduncles and an abnormally deep interpeduncular fossa.[5] At present, 4 genes causative of JS have been identified (JBTS3-AHI1 on chromosome 6q23.3, JBTS4-NPHP1 on chromosome 2q13, JBTS5-CEP290 on chromosome 12q21.3, and JBTS6-MKS3 on chromosome 8q24), and 2 additional loci have been mapped (JBTS1 to chromosome 9q34.3 and JBTS2 to chromosome 11p12-q13.3).[6-16] The currently known genes or gene loci account for less than 50% of patients.

Two previous neuropathologic reports[17,18] described an almost complete absence of pyramidal tract decussation in the caudal medulla and an abnormal decussation of the superior cerebellar peduncles. Moreover, a further study[19] also showed a failure of the superior cerebellar peduncles to decussate in the mesencephalon in 2 patients. Lee et al[20] showed thickened superior cerebellar peduncles but did not demonstrate the absence of decussation of the superior cerebellar peduncles. Lee et al[20] and Widjaja et al[19] applied diffusion tensor imaging (DTI), a relatively new MR imaging technique that allows examination of the course and integrity of white matter tracts in vivo.

Received February 15, 2007; accepted after revision April 9.

From the Departments of Pediatric Neurology (A.P., E.B.), and Diagnostic Imaging and MR Center (T.L., K.I., T.A.G.M.H.), University Children's Hospital, Zurich, Switzerland; Department of Neurogenetics (E.M.V., F.B.), CSS-Mendel Institute, Rome, Italy; Department of Diagnostic Radiology (K.I.), Section of Medical Physics, University of Freiburg, Germany; and the Division of Pediatric Radiology (T.A.G.M.H.), Russell H. Morgan Department of Radiology and Radiological Sciences, The Johns Hopkins University School of Medicine, Baltimore, Md.

Please address correspondence to Thierry A.G.M. Huisman, MD, Pediatric Radiology, The Russell H. Morgan Department of Radiology and Radiological Science, Johns Hopkins Hospital, 300 N. Wolfe St, Nelson B-173, Baltimore, MD 21287-0842; e-mail: thuisma1@jhmi.edu

DOI 10.3174/ajnr.A0703

However, in JS the failure of fibers to cross the midline is not a generalized pathologic feature, because the fibers within the optic chiasm, corpus callosum, and other decussating pathways are not affected. Ferland et al[7] found that AHI1 mRNA is expressed in the cell bodies that give rise to axonal tracts that fail to decussate in JS, such as the neuronal cells of the deep-layer V cerebral cortical neurons that give rise to the corticospinal tract that decussates in the medullary pyramids. These results suggest that AHI1 may have a crucial role in the modulation of axonal decussation.

The aim of our study was to extend the previously reported neuropathologic and neuroradiologic findings by 1) studying a larger group of patients (n = 6) with JS, 2) evaluating the decussation of both the superior cerebellar peduncles and pyramidal tracts, and 3) correlating the imaging findings with the results of the genetic mutation analysis. We hypothesized that neuroimaging findings do not differ between the genetic forms of JS.

Patients and Methods

There were 6 patients with JS from 5 families who participated in this study. Clinical and genetic findings are summarized in Table 1. A brother of patient 6 was also affected but was unable to cooperate. All affected subjects had mild to moderate cognitive impairment. They were able to undergo MR imaging without sedation. Parents and patients were informed about the MR examination and consented to participate.

We performed MR imaging using a 3T MR imaging-unit (GE Healthcare, Milwaukee, Wis) and acquired the imaging with a standard 8-channel head coil. Before DTI measurement, we measured conventional sagittal and axial T2-weighted fast spin-echo and coronal T1-weighted spin-echo imaging sequences using standard departmental imaging protocols. Axial imaging was performed in accordance with an imaging plane parallel to the anteroposterior commissural line. We sampled the diffusion tensor by repeating a diffusion-weighted single-shot spin-echo echo-planar sequence along 20 different geometric directions. Diffusion sensitization was achieved with 2 balanced diffusion gradients centered around the 180° radio-frequency pulse. To reduce eddy current effects, we divided the diffusion gradients into 4 alternating-sign gradient lobes, all with the same gradient magnitude.[21] An effective b-value of 1000

Table 1: Clinical and genetic findings in 6 patients with Joubert syndrome (JS)

Patient	1	2	3	4*	5*	6
Age (y)	27	26	26	18	16	10
Origin	Swiss	Swiss	Swiss	Turkish	Turkish	Swiss
Parental consanguinity	+	−	−	+	+	+
CNS	AT, OMA, CI	AT, OMA, CI	AT, OMA, CI	AT, OMA, CI	AT, OMAb, CI	AT, OMA, CI
Features						
Ocular	PR	nor	nor	PR	PR	nor
Kidney	nor	nor	nor	NPHP	NPHP	nor
Genetic form	JBTS3	not known	not known	JBTS5	JBTS5	JBTS1

Note:— + indicates present; −, absent; AT, ataxia; OMA, ocular motor apraxia; CI, cognitive impairment; PR, pigmentary retinopathy; NPHP, nephronophthisis; nor, normal.
* Siblings.

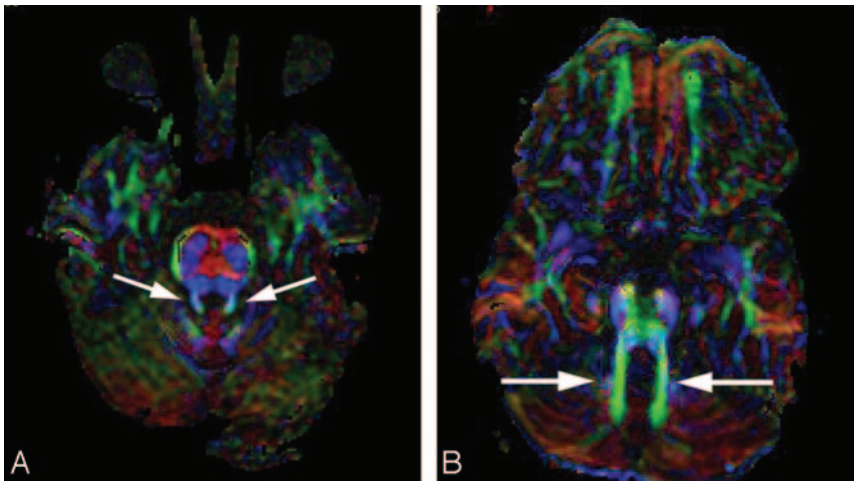

Fig 1. Color-coded FA-maps at the level of the superior cerebellar peduncles. *A,* In a healthy subject, the fibers within the superior cerebellar peduncles have a slight vertical orientation, characterized by a blue color coding on color-coded FA-maps, confirming the vertical orientation of the fibers within the superior cerebellar peduncles (*arrows*). *B,* In JS, the fibers in the superior cerebellar peduncles have a more horizontal orientation, confirmed by the green color coding of the superior cerebellar peduncles on color vector DTI (*arrows*).

s/mm^2 was used for each of the 20 diffusion-encoding directions. We performed an additional measurement without diffusion weighting (b = 0 s/mm^2). Scan parameters were TR, 8,000 ms; TE, 91 ms; matrix size, 128 × 120 mm; and FOV, 256 × 240 mm. A total of 36 contiguous 3-mm-thick axial sections were acquired, covering the caudal medulla up to the vertex. We sampled each diffusion tensor 6 times to optimize the signal-to-noise ratio (SNR). We generated isotropic diffusion-weighted, ADC, and fractional anisotropy (FA) maps using postprocessing software (FuncTool; GE Healthcare). We calculated apparent diffusion coefficient (ADC) maps on a pixel-by-pixel basis using a 2-point (b = 0 and b = 1000 s/mm^2) monoexponential fit approach. The FA maps were calculated as the ratio of the anisotropic component of the diffusion tensor to the whole diffusion tensor, as published previously by Basser and Pierpaoli.[22] The principal 3D orientation of the major eigenvector was color coded per voxel according to the red-green-blue convention, red indicating a predominant left-right (x-element), green an anteroposterior (y-element), and blue a superior-inferior (z-element) orientation of the anisotropic component of diffusion within each voxel. The color intensity scale was proportional to the measured FA-value.

For fiber tractography (FT), we transferred the DTI dataset to a personal computer. We performed fiber tractography using homemade routines based on commercially available image display software (MatLab 6.5; MathWorks, Natick, Mass). Color-coded FA-maps were used to guide placement of the seed points of fiber tracking. Correct positioning of the seed points was also checked on images without diffusion weighting (b = 0 s/mm^2). We achieved 3D FT by positioning connecting seed points along the fiber tracts studied. We studied the superior cerebellar peduncles by positioning seed points within the dentate nuclei and the ipsilateral and contralateral nucleus ruber. Additional seed points were also positioned within the mesencephalon adjacent to the interpeduncular fossa. We studied the corticospinal tracts by positioning seed points bilaterally within the internal capsule. The threshold value for termination of fiber tracking was less than 0.3 for FA and greater than 45° for the trajectory angles between the diffusion tensor ellipsoids. Color-coded FA-maps were evaluated for the presence or absence of a "focal red dot" within the anterior mesencephalon adjacent to the interpeduncular fossa. Absence of the "focal red dot" was interpreted as an absence of a decussation of the fiber tracts within the superior cerebellar peduncles, respectively, as an absence of the decussatio pedunculorum cerebellarium superiorum. In a similar fashion, we studied the caudal medulla oblongata for a "focal red dot" corresponding to the decussation of the corticospinal tracts. We performed FT to confirm the findings of color-coded FA-maps and identify a possible aberrant course of the studied tracts.

Results

In all patients, conventional MR imaging showed the classic MTS with a deep interpeduncular fossa, thickened superior cerebellar peduncles, a widened fourth ventricle, and hypoplasia of the cerebellar vermis. In 5 patients, only the superior cerebellar vermis (until the fissura prima) was present, whereas in the remaining patient the cerebellar vermis was present as far as the fissura secunda. The remnant of the vermis was normal in 1 patient, dysplastic in 2 patients, and questionably dysplastic in 3 patients. All patients showed an elongated mesencephalon, a narrowed isthmus, and a normal quadrigeminal plate and pons. In 1 patient, heterotopic gray matter was identified within the mesencephalon. In 1 patient, the T2-hyperintensity of the cerebellar white matter was slightly increased. In 1 patient, the pituitary gland was hypoplastic (clinically asymptomatic) and in another patient, questionably hypoplastic. No patients showed supratentorial midline anomalies or polymicrogyria.

In all patients, DTI showed that the fibers in the superior cerebellar peduncles were oriented horizontally as represented by a green color coding on the FA-maps, in contrast to the

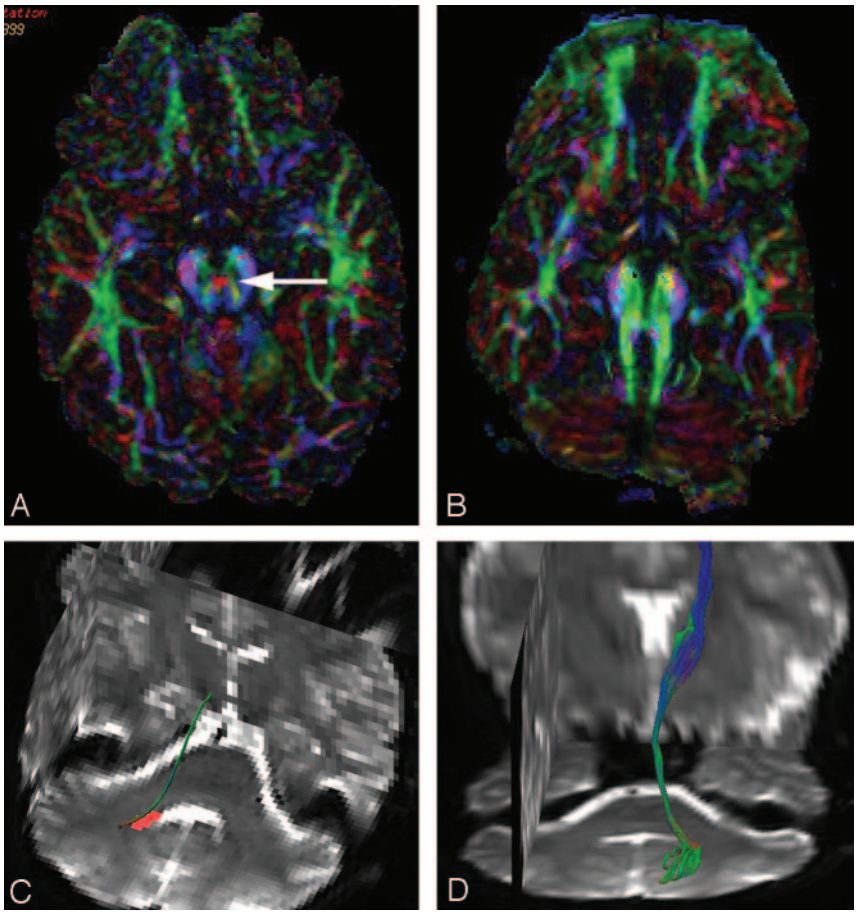

Fig 2. Color-coded FA-maps at the level of the decussation of the superior cerebellar peduncles. *A,* In a healthy subject, on the color-coded FA-maps the decussation of the superior cerebellar peduncles is identified as a "red dot" (*arrow*) at the level of the inferior colliculi of the midbrain. The decussating fibers have a transverse orientation and consequently show a "red color coding." *B,* In JS, the absence of the "red dot" on color-coded FA-maps within the midbrain confirms the failure of the superior cerebellar peduncles to decussate. *C,D,* Fiber tractography displays that, in JS, the fibers within the superior cerebellar peduncles that connect the dentate nucleus with the nucleus ruber do not cross and remain ipsilateral. Axial, coronal, and sagittal anatomic T2-weighted images are projected within the display for orientation purposes.

slight vertical orientation (blue color coding) in healthy control subjects (Fig 1*A, B*). Furthermore, in all patients these fibers projected into the red nuclei and thalami without decussating. This was demonstrated by absence of the transverse fibers at the level of the inferior colliculi of the midbrain, as absence of the characteristic "focal red dot" deep within the interpeduncular fissure on color-coded FA-maps (Fig 2*A, B*). Failure of the superior cerebellar peduncles to decussate was also demonstrated by FT (Fig 2*C, D*). The deep cerebellar nuclei (dentate nuclei) also appeared abnormal because they were located more laterally in 5 patients (Fig 3), whereas in the remaining patient they were questionably lateralized. The corticospinal tract showed no decussation in the caudal medulla in all the patients. Failure of decussation was demonstrated by the absence of the transverse fibers at this level, as absence of a "focal red dot" on color-coded FA-maps (Fig 4*A, B*), and was also visualized by FT (Fig 4*C*). For reasons of comparison, FT with multiple crossing tracts is displayed in a healthy subject (Fig 4*D*). The results are summarized in Table 2.

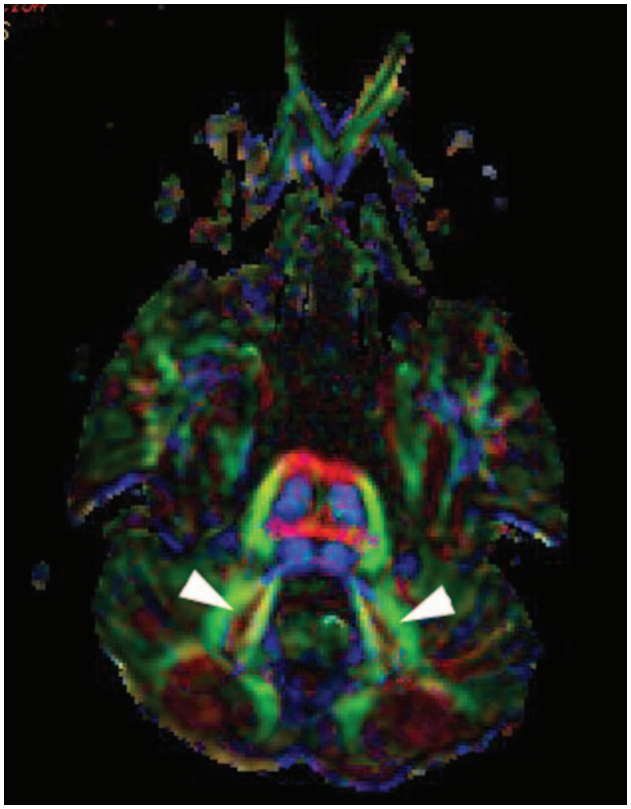

Fig 3. Color-coded FA-maps at the level of the dentate nuclei. In JS, the dentate nuclei are significantly lateralized (*arrowheads*).

Discussion

JS is an autosomal-recessive inherited complex malformation of the hindbrain. Well-known features include the hypoplasia or aplasia of the cerebellar vermis and the MTS. Previous neuropathologic findings also showed an almost complete absence of pyramidal decussation.[17,18] Furthermore, Yachnis and Rorke[18] found only a rudimentary decussation of the superior cerebellar peduncles, which was not described by Friede and Boltshauser.[17]

With conventional MR images, Sener[23] found an abnormal signal intensity in the decussation of the superior cerebellar peduncles in 1 patient with JS. In a study by Parisi et al,[24] a functional MR imaging study demonstrated that 1 patient with JS showed a striking bilateral activation of the sensorimotor and cerebellar cortex, in contrast to the typical highly lateralized activation seen in control subjects. This abnormal activation pattern suggested altered functional organization in the brain related to anatomic differences such as abnormal decussation of the corticospinal tracts. DTI and fiber tractography are new methods that can demonstrate the orientation of fiber pathway. Using DTI and tractography in 3 patients

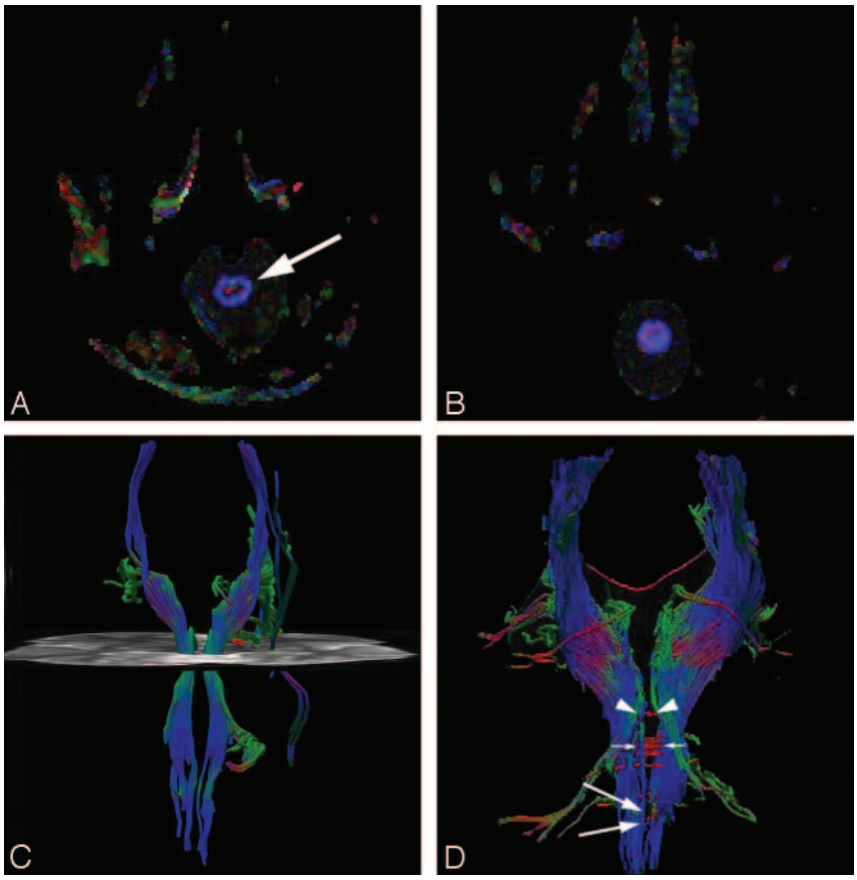

Fig 4. Color-coded FA-maps of the decussation of the pyramidal tracts. *A,* In a healthy subject, the transverse orientation of the decussating fibers of the pyramidal tracts can be identified as a "red dot" within the caudal medulla (*arrows*). *B,* In JS, the "red dot" is missing, indicating that the pyramidal tracts do not cross within the caudal medulla. *C,* Fiber tractography displays the course of the pyramidal tracts (*blue encoded*) in a coronal projection. No crossing fibers could be identified, and the pyramidal tracts show a parallel course within the caudal medulla. A group of the noncrossing fibers within the superior cerebellar peduncles are also displayed on the left side (*green encoded*). An anatomic axial section is projected within the display for orientation purposes. *D,* In a healthy subject, fiber tractography displays the normal course of the pyramidal tracts (*blue encoded*) in a coronal projection. A partially red-encoded pyramidal decussation is seen at the level of the caudal medulla (*large arrows*). The red-encoded decussation of the superior cerebellar peduncles is seen at the level of the mesencephalon (*arrowheads*). In addition, multiple red-encoded crossing fibers are seen at the level of the pons (*small arrows*).

Table 2: Structural MR and diffusion tensor imaging findings in six patients with Joubert syndrome

Patient	Vermis	MTS	Superior Cerebellar Peduncles		Location of the Deep Cerebellar Nuclei	Pyramidal Tract Decussation
			Decussation	Configuration		
1	<1/3*	+	−	Horizontal	Lateralized	−
2	<1/3*	+	−	Horizontal	Lateralized	−
3	<1/3*	+	−	Horizontal	Lateralized	−
4	<1/3*	+	−	Horizontal	Lateralized	−
5	<2/3†	+	−	Horizontal	Quest, lateralized	−
6	<1/3*	+	−	Horizontal	Lateralized	−

Note:—+ indicates present; −, absent; MTS, molar tooth sign; quest., questionably.
* Cerebellar vermis present only as far as the fissura prima.
† Cerebellar vermis present only as far as the fissura secunda.

with JS, Lee et al[20] showed thickened superior cerebellar peduncles. Also, by using DTI and tractography in 2 patients with JS, Widjaja et al[19] found horizontally oriented superior cerebellar peduncles that failed to decussate and laterally located deep cerebellar nuclei.

In our study, we confirmed and extended these findings by studying 6 patients with JS. DTI and tractography showed the absence of decussation of the superior cerebellar peduncles and the more lateral localization of the deep cerebellar nuclei. In addition, we could confirm the neuropathologic findings of the absence of the decussation of the corticospinal tract. To our knowledge, that has not previously been shown by neuroimaging methods.

The findings of Parisi et al[24] suggested at least some degree of decussation of the superior cerebellar peduncles and of the corticospinal tract. The findings of Widjaja et al,[19] as well as of our results, showed a complete absence of decussation of these pathways. We believe that this difference can be ascribed to the well-known heterogeneity of JS.

In addition, we correlated these findings with mutation analysis. Ferland et al[7] found that AHI1 mRNA is mainly expressed in the neurons, which give rise to axonal tracts that fail to decussate at the midline in JS, such as the neurons of the cerebellar dentate nucleus that send axons across the midline, forming the superior cerebellar peduncles, and also in the neurons of the deep-layer V cerebral cortical neurons, which give rise to the corticospinal tract that decussates in the medullary pyramids.

They concluded that AHI1 may be a crucial cell-autonomous modulator of axonal decussation.[7] Remarkably, we found absence of decussation of the superior cerebellar peduncles and pyramidal tracts not only in 1 patient with AHI1 mutation, but also in the 5 patients without AHI1 mutation (2 patients with CEP290 mutation, 1 with linkage to the locus on chromosome 9, and 2 other patients in whom the mutation is

not yet known). This observation suggests that the identical neuroimaging findings represent a "final morphologic pathway" for the various genetic JS mutations (ie, the normal axonal decussation not only requires normal AHI1 gene function but also depends on the integrity of other genes).

Failure of decussation of the superior cerebellar peduncles and corticospinal tract is not specific to JS. In the autosomal-recessive syndrome of horizontal gaze palsy and progressive scoliosis (HGPPS), Jen et al[25] found the absence of the decussation of the corticospinal tract by using evoked potentials. Using DTI, Sicotte et al[26] confirmed these results and also showed the absence of the decussation of the superior cerebellar peduncles. However, HGPPS is not associated with the MTS but may show a longitudinal cleft of the brain stem. From a clinical standpoint, the 2 syndromes are completely different: the patients with HGPPS do not demonstrate the severe ataxia and apraxia typical of JS, and their major disability arises from progressive scoliosis. From a genetic standpoint, the 2 syndromes are also different because ROBO3, the gene responsible for HGPPS, is located on chromosome 11q23–25.

We are aware that our study had limitations. The number of patients seemed small, but, with an estimated prevalence of 1:100,000, recruiting of patients with JS capable of cooperating sufficiently was very difficult. However, the patients were not sufficiently cooperative to perform functional MR imaging or transcranial magnetic stimulation. Because almost all patients survive well into adulthood, confirmation of pathologic findings is not possible. Finally, the question should be raised if the current resolution of DTI and FT is good enough to differentiate between complete absence versus a significantly decreased volume of decreased commissural fibers in patients with more severe or milder forms of JS. In addition, the current resolution of DTI and the limited knowledge about aberrant, or so-called compensatory, fiber tracts in JS represented additional limitations that could be solved by future ultrahigh-resolution DTI sequences.

Conclusion

In 6 patients with JS, we found, independent of the genetic background, the absence of decussation of the superior cerebellar peduncles and of the corticospinal tract. Furthermore, in all patients, the superior cerebellar peduncles were oriented horizontally, and in 5 patients, the deep cerebellar nuclei were located more laterally.

Acknowledgments

The first author (A.P.) was financially supported by a donation from the United Bank of Switzerland (UBS). This donation was made at the request of an anonymous client.

References

1. Joubert M, Eisenring JJ, Robb JP, et al. **Familial agenesis of the cerebellar vermis. A syndrome of episodic hyperpnea, abnormal eye movements, ataxia, and retardation.** *Neurology* 1969;19:813–25
2. Boltshauser E, Isler W. **Joubert syndrome: episodic hyperpnea, abnormal eye movements, retardation and ataxia, associated with dysplasia of the cerebellar vermis.** *Neuropadiatrie* 1977;8:57–66
3. Saraiva JM, Baraitser M. **Joubert syndrome: a review.** *Am J Med Genet* 1992;43:726–31
4. Satran D, Pierpont ME, Dobyns WB. **Cerebello-oculo-renal syndromes including Arima, Senior-Löken and COACH syndromes: more than just variants of Joubert syndrome.** *Am J Med Genet* 1999;86:459–69
5. Maria BL, Hoang KB, Tusa RJ, et al. **"Joubert syndrome" revisited: key ocular motor signs with magnetic resonance imaging correlation.** *J Child Neurol* 1997;12:423–30
6. Lagier-Tourenne C, Boltshauser E, Breivik N, et al. **Homozygosity mapping of a third Joubert syndrome locus to 6q23.** *J Med Genet* 2004;41:273–77
7. Ferland RJ, Eyaid W, Collura RV, et al. **Abnormal cerebellar development and axonal decussation due to mutations in AHI1 in Joubert syndrome** [published erratum appears in *Nat Genet* 2004;36:1126]**.** *Nat Genet* 2004;36:1008–13
8. Dixon-Salazar T, Silhavy JL, Marsh SE, et al. **Mutations in the AHI1 gene, encoding jouberin, cause Joubert syndrome with cortical polymicrogyria.** *Am J Hum Genet* 2004;75:979–87
9. Parisi MA, Bennett CL, Eckert ML, et al. **The NPHP1 gene deletion associated with juvenile nephronophthisis is present in a subset of individuals with Joubert syndrome.** *Am J Hum Genet* 2004;75:82–91
10. Castori M, Valente EM, Donati MA, et al. **NPHP1 gene deletion is a rare cause of Joubert syndrome related disorders.** *J Med Genet* 2005;42:e9
11. Sayer JA, Ottro EA, O'Toole JF, et al. **The centrosomal protein nephrocystin-6 is mutated in Joubert syndrome and activates transcription factor ATF4.** *Nat Genet* 2006;38:674–81
12. Valente EM, Silhavy JL, Brancati F, et al. **Mutations in CEP290, which encodes a centrosomal protein, cause pleiotropic forms of Joubert syndrome.** *Nat Genet* 2006;38:623–25
13. Baala L, Romano S, Khaddoour R, et al. **The Meckel-Gruber syndrome gene, MKS3, is mutated in Joubert syndrome.** *Am J Hum Genet* 2007;80:186–94
14. Saar K, Al-Gazali L, Sztriha L, et al. **Homozygosity mapping in families with Joubert syndrome identifies a locus on chromosome 9q34.3 and evidence for genetic heterogeneity.** *Am J Hum Genet* 1999;65:1666–71
15. Valente EM, Salpietro DC, Brancati F, et al. **Description, nomenclature, and mapping of a novel cerebello-renal syndrome with the molar tooth malformation.** *Am J Hum Genet* 2003;73:663–70
16. Keeler RC, Marsh SE, Leeflang EP, et al. **Linkage analysis in families with Joubert syndrome plus oculo-renal involvement identifies the CORS2 locus on chromosome 11p12–q13.3.** *Am J Hum Genet* 2003;73:656–62
17. Friede RL, Boltshauser E. **Uncommon syndromes of cerebellar vermis aplasia. I: Joubert syndrome.** *Dev Med Child Neurol* 1978;20:758–63
18. Yachnis AT, Rorke LB. **Neuropathology of Joubert syndrome.** *J Child Neurol* 1999;14:655–59; discussion 669–72
19. Widjaja E, Blaser S, Raybaud C. **Diffusion tensor imaging of midline posterior fossa malformations.** *Pediatr Radiol* 2006;36:510–17
20. Lee SK, Kim DI, Kim J, et al. **Diffusion-tensor MR imaging and fiber tractography: a new method of describing aberrant fiber connections in developmental CNS anomalies.** *Radiographics* 2005;25:53–65; discussion 66–68
21. Reese TG, Heid O, Weisskoff RM, et al. **Reduction of eddy-current-induced distortion in diffusion MRI using a twice-refocused spin echo.** *Magn Reson Med* 2003;49:177–82
22. Basser PJ, Pierpaoli C. **Microstructural and physiological features of tissues elucidated by quantitative-diffusion-tensor MRI.** *J Magn Reson B* 1996;111:209–19
23. Sener RN. **MR imaging of Joubert's syndrome.** *Comput Med Imaging Graph* 1995;19:481–86
24. Parisi MA, Pinter JD, Glass IA, et al. **Cerebral and cerebellar motor activation abnormalities in a subject with Joubert syndrome: functional magnetic resonance imaging (MRI) study.** *J Child Neurol* 2004;19:214–18
25. Jen JC, Chan WM, Bosley TM, et al. **Mutations in a human ROBO gene disrupt hindbrain axon pathway crossing and morphogenesis.** *Science* 2004; 304:1509–13
26. Sicotte NL, Salamon G, Shattuck DW, et al. **Diffusion tensor MRI shows abnormal brainstem crossing fibers associated with ROBO3 mutations.** *Neurology* 2006;67: 519–21